ANALYSES OF DIRECT PATH, LOW FREQUENCY, MONOSTATIC REVERBERATIONS FROM EXPOSED ROCKS AND SEDIMENT COVERED AREAS OF THE ARSRP FINE-SCALE EXPERIMENT

Ashok K. Kalra (1) and James K. Fulford (2)

(1) Naval Research Laboratory *, Stennis Space Center, MS 39529-5004
* current address: Naval Oceanographic Office, Stennis Space Center, MS 39522-5001
(2) Naval Research Laboratory, Stennis Space Center, MS 39529-5004

INTRODUCTION

In 1989, Office of Naval Research (ONR) initiated Acoustic Reverberation Special Program (ARSRP) with the objective to study the sea bottom/subbottom reverberation (scattering) hypothesis at low frequencies (50 - 500 Hz) and low grazing angles (15°). Consequently, in Summer of 1993, ARSRP acquired extensive amount of acoustic reverberation data, along with environmental (acoustic and nonacoustic) data, at three well-defined sites within the ONR Atlantic Natural Laboratory (Mid-Atlantic Region between Kane and Atlantis fracture zones). These data are in addition to the ARSRP reconnaissance experiment that was conducted along the acoustic reverberation corridor in Summer of 1991 (ARSRP, 1991). We discuss the analyses of a part of the ARSRP acoustic reverberation data that were acquired in the fine-scale experiment (in Summer of 1993).

Most of the ARSRP fine-scale experiment acoustic reverberation data were acquired with bottom moored vertical arrays (at specific sites of interest), and towed horizontal arrays (close to the sea surface) using standard ARSRP configurations. Additional acoustic reverberation data were also acquired with Naval Research Laboratory's Deep Towed Acoustic/Geophysical System (DTAGS). We have analyzed DTAGS acoustic array (reverberation) data that were acquired when DTAGS was towed horizontally close to the sea bottom and determined the scattering strength versus grazing angle and frequency relations. The scattering strengths vs grazing angles (corrected for local slopes) relations are similar to Lambert's law with some variations. We have also determined the reverberation process to be selective facet backscattering (Dyer et al., 1993).

DATA ACQUISITION

DTAGS is designed to acquire two different sets of data simultaneously with two collinear horizontally towed line arrays (i.e., acoustics and geophysics) under nominal operating conditions. The geophysics data are used to map the bottom and subbottom features. The acoustic array data constitutes the direct path reverberation data that we have analyzed.

Independently, DTAGS can also acquire data when the acoustic array is towed as a vertical line array (at very slow speeds) in a separate pass. Such data were also acquired for the ARSRP fine-scale experiment, but these data will not be used in this analysis.

DTAGS is identical to a conventional seismic streamer except that it is designed to acquire data at frequencies (250 to 650 Hz) higher than normally used in seismic acquisitions, and it can be towed in a near bottom configuration in deep waters (depths to 5000 m). The system consists of both the towed receiving arrays, and its own self contained high frequency single element source that is towed at the same operating depth as the receive arrays. The source signal is 125 ms linear frequency modulated (LFM) chirp with a frequency bandwidth ranging from 250 to 650 Hz. DTAGS acoustic array data that are analyzed here were acquired by towing the instrument from 300 to 1100 m from the seafloor in water depths of 4400 m.

The DTAGS acoustic array consisted of 24 receiver groups spaced 2.1 m apart. The near offset distance from the source to the first group was 72 m. A single hydrophone receiver, located 59 m from the source was used to recorded the source signature for each transmission. The acoustic data was recorded for 4.536 s at a sampling rate of 2315 samples per second. DTAGS data were acquired in conjunction with other acoustic data collected by other vessels in a time sharing fashion. Consequently, DTAGS acquired data every 12 minutes for a duration of 2 minutes. This corresponds to approximately 4 to 5 contiguous pings for each operating period.

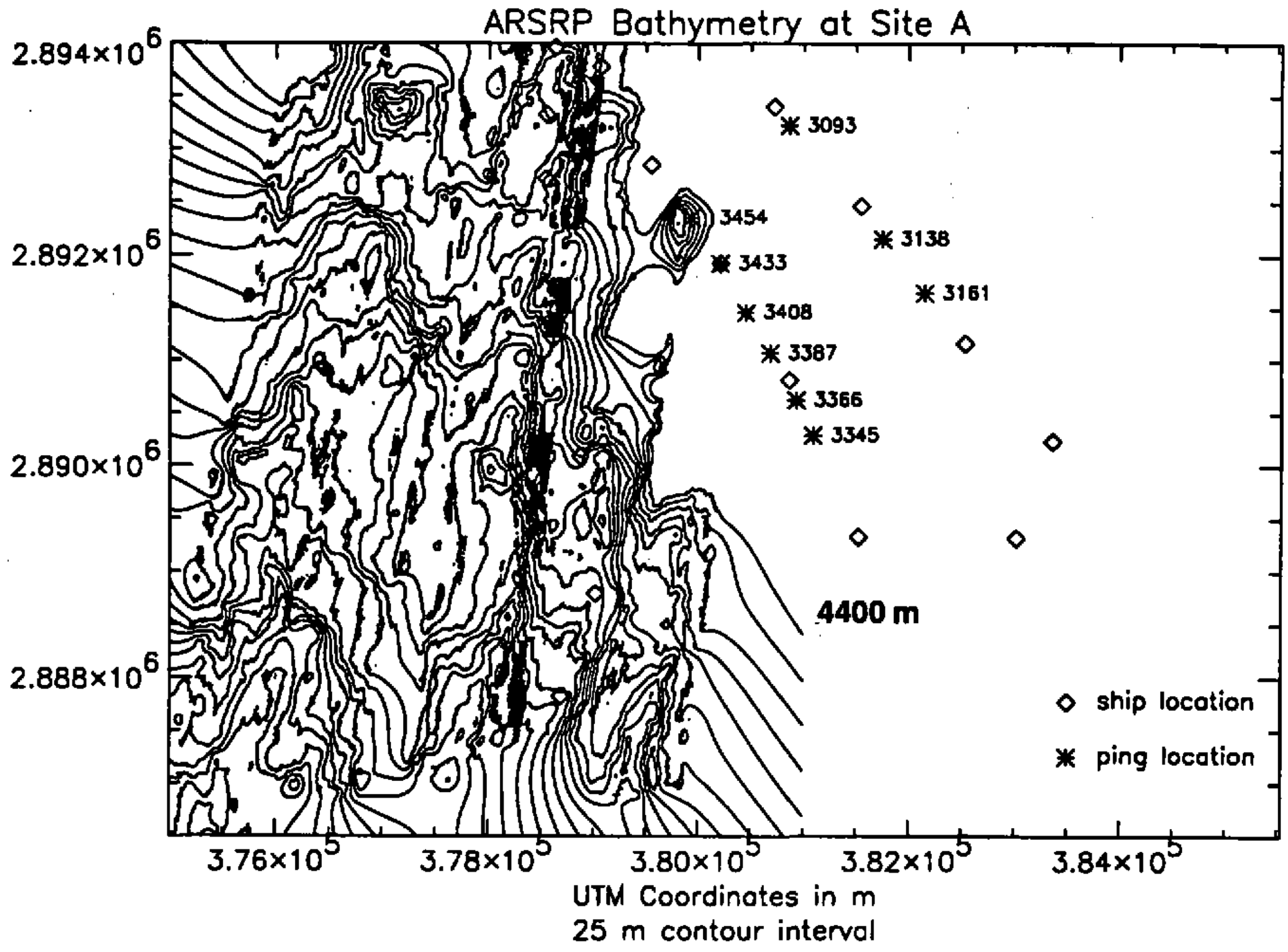

Figure 1. Plot of ASARP site A bathymetry showing the ping locations used in this analysis.

Figure 1 indicates the ship tract and the ping locations for the DTAGS data at ARSRP Site A that are analyzed here. Due to a lack of transponder equipment on the DTAGS instrument, the exact location of each ping is not known. The ping locations had to be estimated from the total length of cable out, the depth of the source, and its distance from the seafloor. We assumed that the cable attained a catenary in shape, and estimated the location of the pings behind the ship. Pings in Figure 1 are such estimations of some selected source locations. In determining these estimates we assumed that the DTAGS source and receiver arrays lay in a straight line behind the tow ship. The pings illustrated in Figure 1 are those which have been selected for analyses, there are others that have not been analyzed and are therefore excluded from the figure. Note that most of the pings in this analysis are located within the sediment pond next to exposed rocks.

DATA PROCESSING

First the data for each ping were deconvolved for the source signature recorded in the field. This compensates for the ping to ping variation in source signature. Next the data were beam formed in the time domain (Kalra and Fulford, 1993) to preserve the high frequencies that were present in the original signal.

There were three depth sensors placed along the array. The sensors were located at the source and the first and the last groups of the acoustic receive array. The depth readings indicate that the receiver array was not parallel to the geoid for the most part of the experiment. For the data analyzed here, the source was always furthest from the sea floor, with the last group nearest and the first group intermediate in depth. We assumed that the array between the first and last group was straight, and determined the inclination of the towed receiver array. For the most part, this inclination was 20°. Later, in order to determine the grazing angles at the bottom with respect to the bottom topography by ray tracing, we corrected the beam formed data for this array inclination.

DATA INTERPRETATION

Figure 2 shows the hydrophone data for ping # 3366. The source signature has been previously deconvolved from the data. Ping # 3366 lies entirely within the sediment pond. The coherent seafloor event is located at 0.82 s (on channel #1) followed by subsurface coherent returns (to 0.92 s) and later some of the broken (less coherent) returns from 0.96 to 1.16 s. At much later times, there are some additional coherent returns at 2.02 s, followed by some broken returns from 2.07 to 2.16 s and further coherent returns at 2.21 and 2.28 s. The coherent returns at 2.02, 2.21, and 2.28 s are interpreted to be selected facet backscattering events as suggested by Dyer et al (1993). Because of the long times involved for these events, they are thought to be scattered from the neighboring exposed rocks and not from any strong acoustic contrasts contained within the sediment cover. It is anticipated that there is little chance of a return from within the sediments to have survived the two way transmission loss expected for these long times. The packet of broken returns 2.07 to 2.16 s are rough interface returns, also from exposed rocks.

Figure 3 is the time-domain beam formed plot of the data shown in Figure 2. These data have not yet been corrected for inclination of the array. The seafloor event is indicated to arrive at beam angle 21° (at 0.82 s) followed by the subsurface coherent events to 0.92 s and later the subsurface broken events (indicated by the hyperbolic spread pattern) as were inferred from the time plot shown in figure 2. Figure 3 also indicates the presence of the later coherent arrivals at 2.02, 2.21, and 2.28 s and broken events from 2.07 to 2.16 s as predicted from the data illustrated in figure 2. The later coherent events appear to arrive at different beam angles varying from 18° to 49° in comparison to the seafloor event (at 21°). The broken returns from 2.07 to 2.16 s arrive at different beams (from 18° to 41°) but at similar times. The coherent events arrive at fixed beam angles namely 32° at 2.02 s and 45° at 2.21 s. The spread of 8° across the events is the beam width of the array.

SCATTERING STRENGTHS

A selected number of facet backscattering events were identified on deconvolved hydrophone data (as outlined above) for each ping analyzed. Consequently, an isolated event for each ping was selected to be further analyzed for scattering strengths. Based on the time arrival, the isolated event was then marked on the corresponding beamformed data along with the associated beam arrival angle. In the beamformed we noticed that the event extended more than a single beam angle. This is due to the beam width of the receive array which is about 8° in the broadside direction for the 24 element array.

The sonar equation (Urick, 1983) was used to determine the scattering strengths. The equation, as used, is:

$$SS = (RL-SL) + 2TL - 10 \log (A) + AG$$

where SS is the scattering strength in dB per square meter, RL is the received reverberation level, SL is the source level, 2TL is the two way transmission loss, A is the insonified area, and AG is the array gain of the receive horizontal array. All of the parameters needed to calculate scattering strengths were derived from the data (or given system parameters) with the exception of the grazing angle at the bottom which was determined from ray tracing. The ray tracing gave the grazing angle to the known regional slope using the high resolution bathymetry shown in Figure 1.

Broad band (250 to 650 Hz) beam formed data, such as illustrated in Figure 3, were first band passed filtered in steps of 50 Hz starting from the 250 to 300 Hz band. This resulted in eight 50 Hz bands. These bands were identified by their center frequencies, the first being 275 Hz. Next we determined the time window of the isolated event from band to band by visual examination, and determined the rms value of the event in dB. This is the reverberation level of the facet backscattered return compensated for source level (RL - SL) due to the fact that the data has already been source signature deconvolved.

The two-way transmission loss were determined from the two-way time of the isolated backscattered event assuming a constant water sound speed of 1540 m/s between the receive array and the sea bottom. The water sound speed was determined from the direct blast times on the deconvolved hydrophone data.

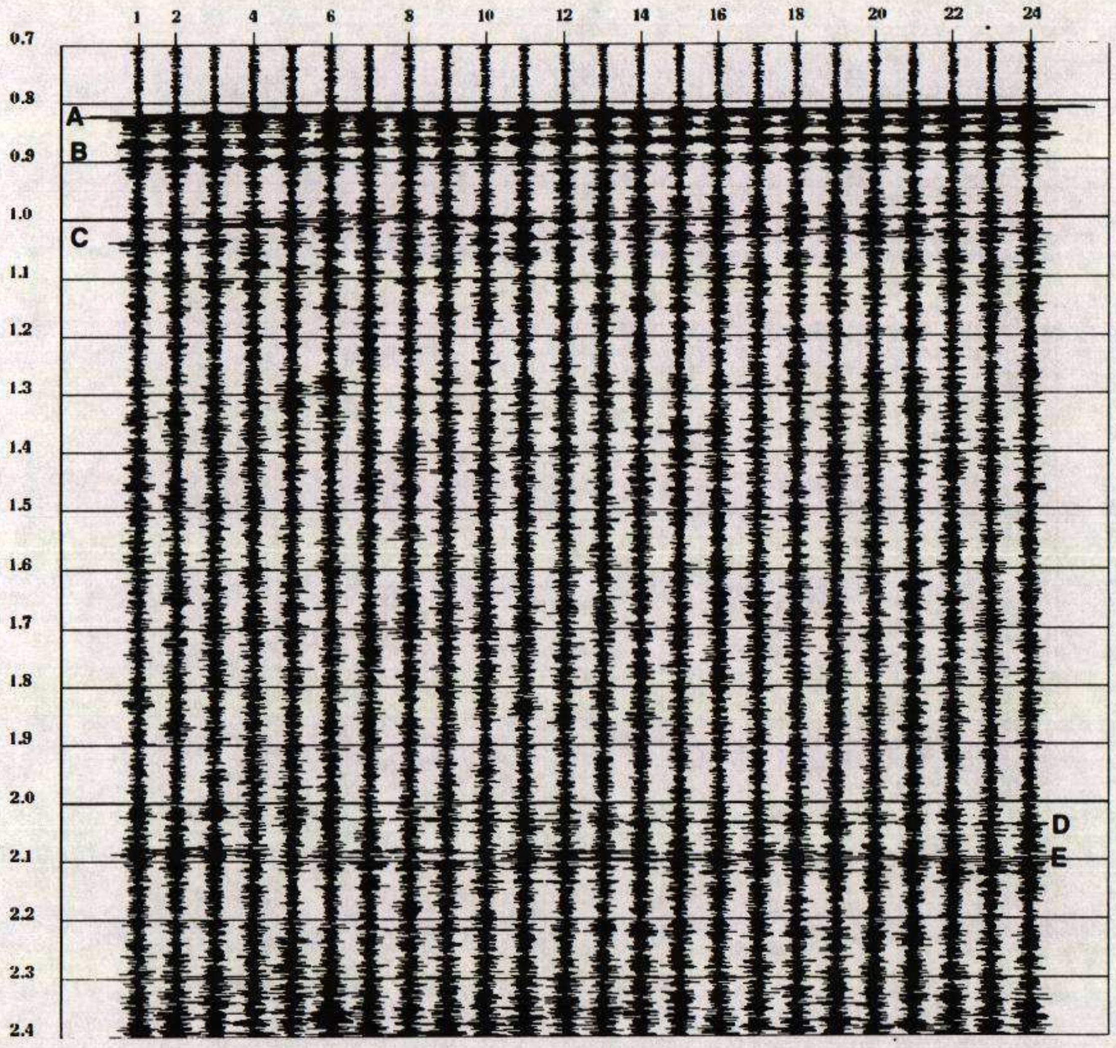

Figure 2. Deconvolved hydrophone data for ping # 3366 showing (A) the seafloor return, (B) subsurface layers, (C) subsurface incoherent scattering, (D) facet scattering from an object on the sea floor, and (E) rough surface scattering from surface topographical features.

The area of the insonfication of the bottom was determined by simple geometric arguments. The cross width of the area was determined from receiver array beam width that was adjusted for the deviation of the beam from the broadside direction, again considering a constant velocity water column. The in-line dimension of the insonfication patch is the time-window of the analysis window of the event.

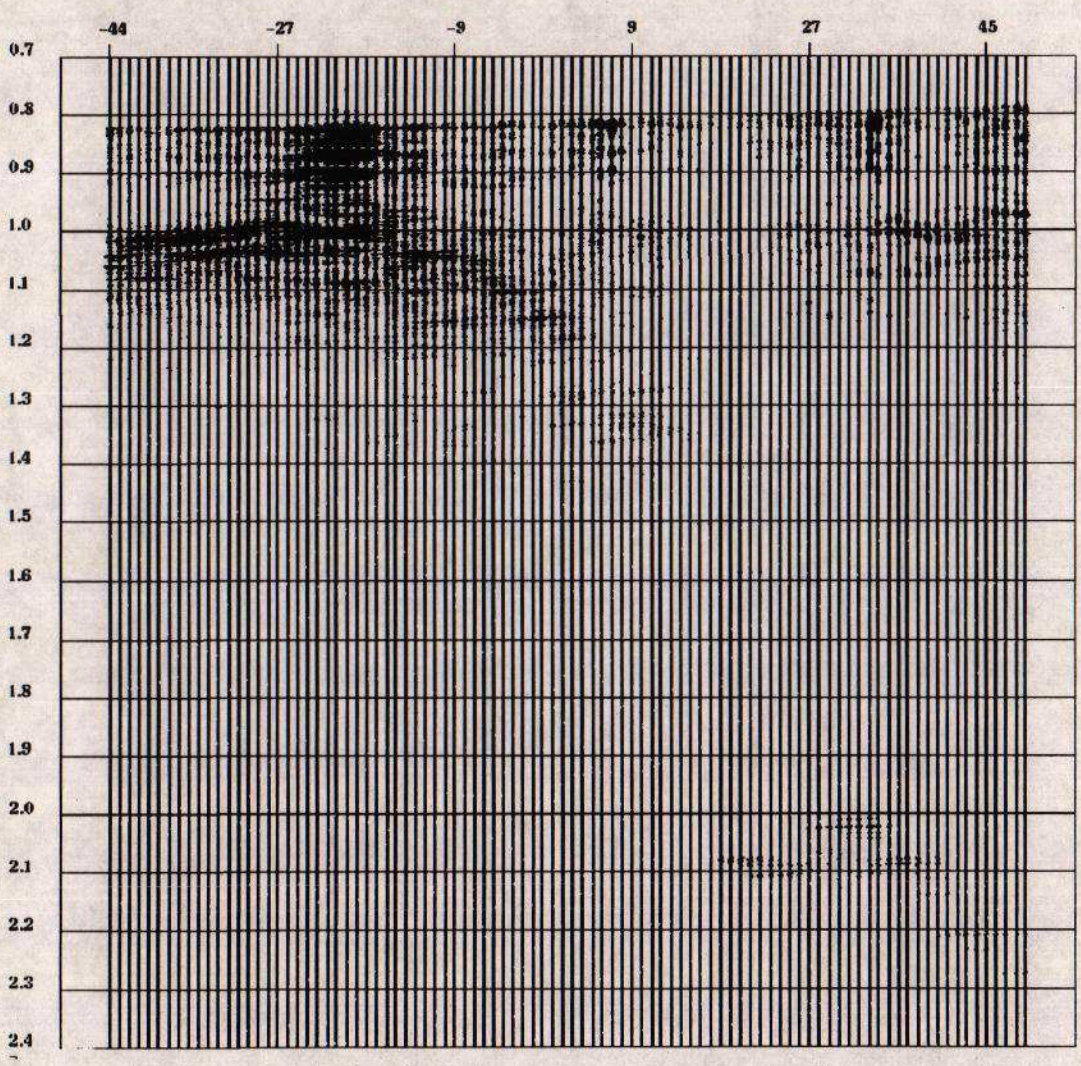

Figure 3. Time domain beamform plot of ping # 3366 (same data as shown in figure 2).

SUBBOTTOM STRUCTURE

One of the goals of the analysis was to determine the strength of subbottom scatterers. We were unable to find any consistent (i.e. ping to ping events that suggested a correlateable scattterer). We did however look at the impedance contrasts (since velocity structure data is unavailable at the time of this analysis) in the surface, and first subsurface layer for regional trends. These contrasts we obtained using plane wave reflection methods applied to the measured coherent seafloor and first subbottom event.

RESULTS AND CONCLUSIONS

Figure 4 is a plot of the scattering strengths vs grazing angles adjusted for the bottom slope for four different grazing angles ranging from 31° to 73° as a function of frequency , for reference a plot of a Lambert curve with a constant of proportionality of 27 dB is also plotted. Note that the scattering strengths are generally increasing with grazing angle, and consitent with Lambert's law. It should be noted that the grazing angles used in this analysis are probably not known to more than 3° for the lowest grazing angles, and 10° for the highest.

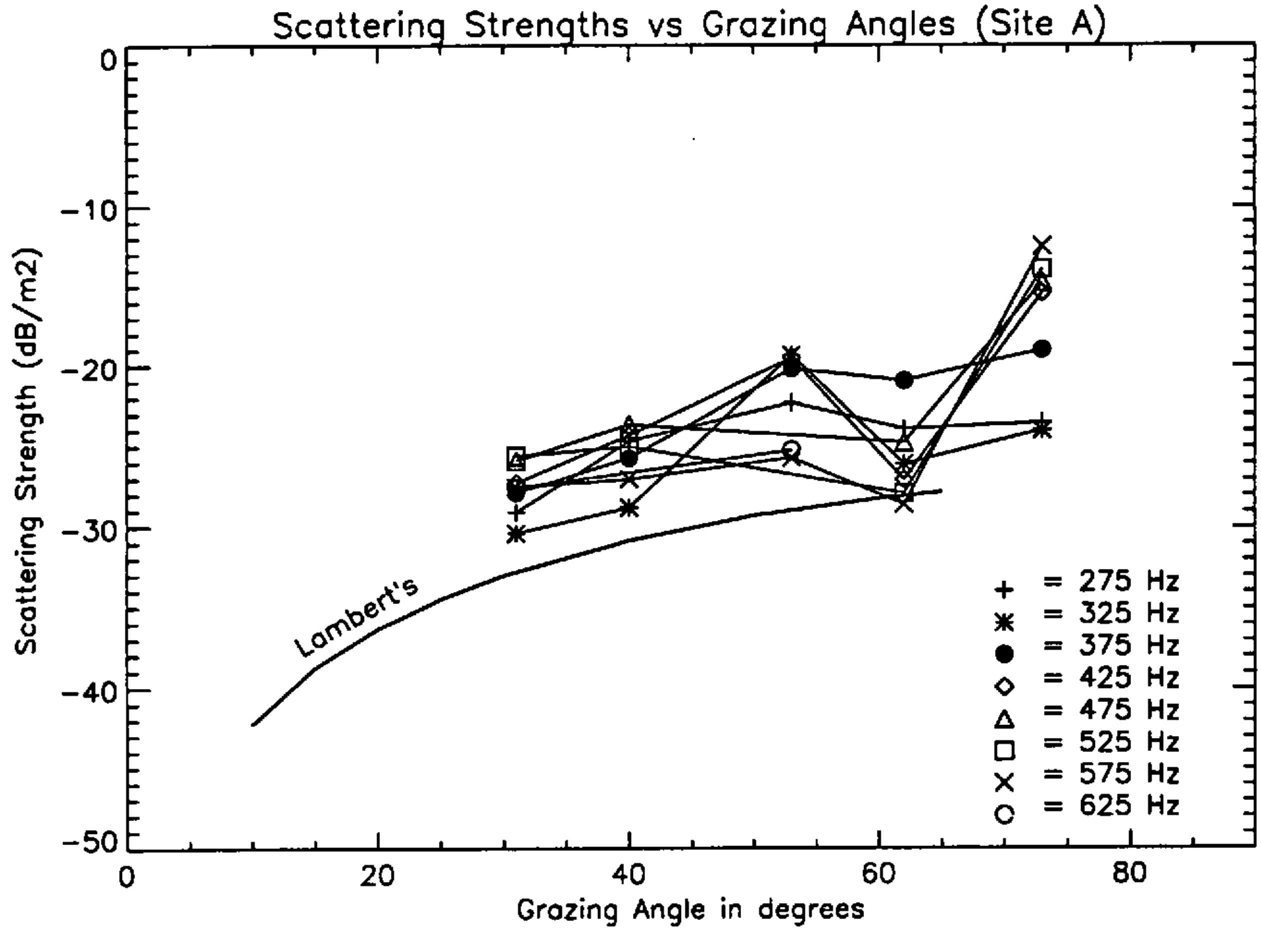

Figure 4. Plot of scattering strength versus grazing angle for the 8 analyzed frequency bins (Lambert's law plot shown for reference).

As noted the DTAGS package lacked high frequency transponder equipment. The position was estimated using the measured depths to the package, the amount of tow cable deployed, and the local topography viewed by the system. We have error in both determining the distance the instrument package is behind the tow vessel, and the amount of off axis motion that the instrument package is undergoing. We have tentatively estimated that our probable circular error in the instrument position is 200 meters. This implies that grazing angle error is minimal for distant events, and maximum for near in events. A second error that arises from the lack of knowledge of the position of the system is an uncertainty over which facet is being insonfied with any given ping. We have analyzed the data assuming that a single family of facets is responsible for the backscattering, clearly this can not be verified with the data we have.

Table 1 shows the derived acoustic impedance relative to sea water for the sea floor, and first subbottom layer for 7 pings. Note that the sea floor impedance is virtually constant over the basin (mean 1.39, standard deviation .03), while the first subbottom layer shows some variation - in particular the subbottom layer seems to have a larger acoustic impedance in a northeasterly direction from the isolated hillock, the two way time interval between the surface and first layer was 42 milliseconds, which may be associated with the hillock.

Table 1. Derived acoustic impedance from analyzed pings.

ping #	3454	3433	3363	3161	3138	3093	3025
sea floor	1.38	1.37	1.42	1.41	1.38	1.33	1.42
first layer	1.94	1.67	1.84	1.77	1.88	1.99	1.901

ACKNOWLEDGMENTS

The data were obtained using the DTAGS system under the direction of Dr. J. Gettrust. This project was supported by the Office of Naval Research, Program Element No. 0601153N, under Program Manager Dr. Mohsen Badiey.

REFERENCES

Acoustic Reverberation Special Research Program Initial Report, 19 August 1991, Acoustic Reconnaissance Cruise prepared for Office of Naval Research.

Dyer, I., A.B. Baggeroer, H. Schmidt, J.R. Fricke, N. Ozluer and D. Giannoni (1993) "Discrete backscatter can be dominant in rough bottom reverberation" in Ocean Reverberation edited by D.D. Ellis, J.R. Preston, and H.G.Urban, Kluwer Academic Publishers.

Kalra, A.K., and J.K. Fulford (1993) "Directional processing of the simulated direct path, broad band reverberation data and its interpretation" in Ocean Reverberation edited by D.D. Ellis, J.R. Preston, and H.G.Urban, Kluwer Academic Publishers.

Urick, Robert J. (1983) Principles of Underwater Sound, McGraw-Hill Book Company.